

# Driving Principles and Hardware Integration of Microrobots Employing Vibration Micromotors

Panagiotis Vartholomeos, Kostas Mougias, and Evangelos Papadopoulos

Department of Mechanical Engineering,  
National Technical University of Athens, 15780 Athens, Greece  
(e-mail: {barthol; egpapado}@central.ntua.gr, kmougias@tee.gr)

**Abstract**— This paper presents a new driving principle for microrobotic platforms whose actuation mechanism is based on two centripetal force actuators. The driving principle results to a controlled motion with precision of a few microns and is suitable for manipulation tasks. The drivers generate an appropriately selected sequence of pulsed actuations resulting in successive microsteps with high repeatability. Simulation results are presented and are compared with experimental results that demonstrate the displacement of a cantilever monitored by a video-microscope. The paper also presents an overview of the hardware assembly process giving emphasis on the integration of the electronic systems and demonstrating the simplicity of the design and the hardware integration process.

**Index Terms**—Micro mechatronic device, micromanipulation, vibration-driven actuation.

## I. INTRODUCTION

During the last decade, microrobotics became an increasingly important field of research and attracted the attention of several research groups of the international robotics community. Domains of application such as micro fabrication, biotechnology, automated microscopy and opto-electronics, demand miniaturized or micro-robotic platforms that provide ultra high precision, flexibility, multi-robot cooperation capability and a wide mobility range [1]. Furthermore, scientists involved in the emerging field of MEMS require a variety of novel tools to probe and manipulate their tiny specimens [2,3]. In order to achieve this, great effort has been put on the design and realization of both micromanipulators and microrobots. Motion principles and actuation mechanisms that combine sub-micrometer motion of high resolution and the speed virtues of coarse positioning have been the subject of extensive studies.

Several micro-actuation techniques have been devised and usually are based on smart materials such as piezoelectric actuators, shape memory alloys, etc. The stick-slip principle [4], implemented using piezoelectric actuators, is the micromotion mechanism employed by most research groups in the field. This principle is used by the MINIMAN microrobot presented in [5]. These platforms are capable for positioning

accuracy better than 200nm and provide velocities of up to a few mm/s. The impact drive principle (a variant of stick-slip principle) is employed by the 3DOF microrobotic platform Avalon, which provides step size of about 3.0  $\mu\text{m}$  and speeds up to 1 mm/s and is presented in [6-7]. A different motion mechanism based on piezo-tubes is utilized by the Nano Walker microrobot, presented in [8]. The first prototypes of this micro-robot were capable of doing minimum steps of the order of 30 nm and demonstrated a maximum displacement rate of 200 mm/s. Possibly MiCRoN is the most advanced example among microrobotic platforms employing piezoelectric actuators. This platform is equipped with an integrated micromanipulator and is presented in [9-10].

Although piezoelectric actuators are arguably the favored smart material for micro-positioning and do provide the required positioning resolution and actuation response, they usually suffer from complex power and driving units, which are prohibitively bulky for tetheredless operation. As a result, integrating the hardware for a cluster of autonomous microrobots employing piezoelectric actuators proves to be a very expensive and challenging task, usually ending with poor results. Moreover, piezoelectric actuators are complex systems that exhibit non-linear behavior and as a result they lack an accurate mathematical model that provides reliable prediction of the system's behavior. The consideration of these issues led to the design of a novel simple and compact microrobot [11] that according to the theory in [12] is able to perform translational and rotational motion, sliding with sub-micrometer positioning accuracy and velocities up to 1.5mm/s. All the components of the mechanism including the electronics are of low cost and readily available.

This paper presents a new driving principle for the platform described in [11,12], which results in a controlled motion with precision of a few microns and is suitable for manipulation tasks. The driving principle is based on an appropriately selected sequence of pulsed actuations, where only one of the two actuators is triggered each time resulting in successive microsteps with high repeatability. Simulation results are presented and are compared with experimental results that demonstrate the displacement of a cantilever monitored by a video-microscope. The paper also presents an overview of the hardware assembly process giving emphasis on the integration

Acknowledgements: This work is co-funded by the European Social Fund (75%) and National Resources (25%) – (EPEAEK II) - HRAKLEITOS

of the miniaturized electronic subsystems. The paper is organized as follows. Section II presents a briefing of the dynamics of the platform and the actuators. Section III refers to the analysis and simulation of the pulsed actuation principle. Section IV gives an overview of the hardware integration and Section V demonstrates experimental results. Finally Section VI presents the conclusions from this work.

## II. MICROROBOT DYNAMICS

### A. Motion principle

The innovative actuation principle of the micro-robot is elaborated in [12]. What follows here is a brief description of the physics that govern the motion. A simplified one dof mobile platform of mass  $M$  is used, whose motion mechanism employs an eccentric mass  $m$ , rotated by a platform mounted motor  $O$ , as shown in Fig. 1. One cycle of operation is completed when the mass  $m$  has described an angle of  $360^\circ$ .

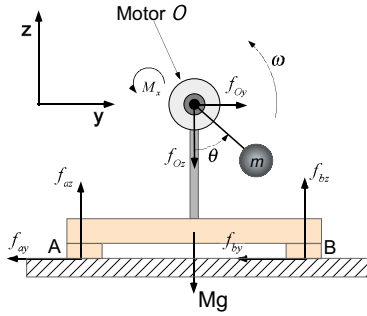


Figure 1. Simplified 1 dof platform with rotating mass  $m$ .

Gravitational and centripetal forces exerted on the rotating mass are resolved along the  $y$ - $z$  axis to yield:

$$\begin{aligned} f_{oy} &= mr\omega^2 \sin\theta \\ f_{oz} &= -mg - mr\omega^2 \cos\theta \end{aligned} \quad (1)$$

where  $g$  is the acceleration of gravity and  $r$  the length of the link between  $m$  and  $O$ . Above a critical value of actuation speed  $\omega_{critical}$  actuation forces overcome frictional forces and motion is induced. The equations of motion of the simplified platform are numerically simulated to yield the results depicted in Fig. 2.

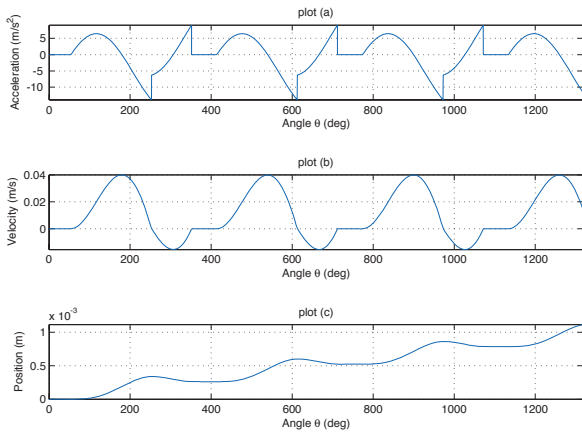


Figure 2. Simulation results for the motion of a 1dof example.

It is clear that for counterclockwise rotation of the eccentric mass  $m$ , the platform exhibits a net displacement towards the positive  $y$ -axis. It has been shown analytically that the motion step the platform exhibits over a cycle of operation, can be made arbitrarily small depending on the actuation speed  $\omega$ , [12]. In practice motion resolution is limited by the electronic driving modules and by the unknown non-uniform distribution of the coefficient of friction  $\mu$  along the surface of the planar motion.

### B. Platform Dynamics

The actuation principle mentioned above was employed to the design of a 2 dof micro-robot as shown in Fig. 3a.

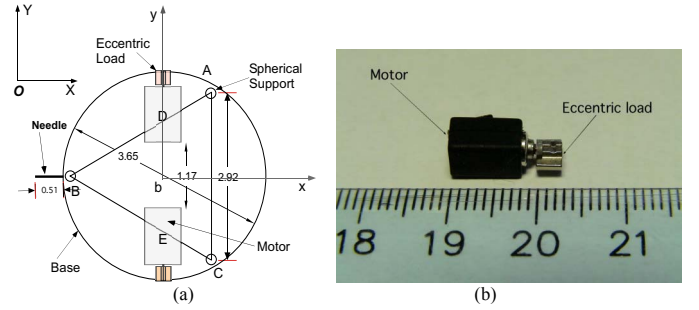


Figure 3. (a) Base design, (b) Actuator.

The platform dynamics are presented in a compact matrix form by the usual Newton Euler equations [13]:

$$M\dot{\mathbf{v}} = \mathbf{R} \sum_i {}^b \mathbf{f}_i, \quad i = \{a, b, c, d, e\} \quad (2a)$$

$${}^b \mathbf{I} \dot{\boldsymbol{\omega}}_p + {}^b \boldsymbol{\omega}_p \times {}^b \mathbf{I} {}^b \boldsymbol{\omega}_p = \sum_i ({}^b \mathbf{r}_i \times {}^b \mathbf{f}_i) + \sum_i {}^b \mathbf{n}_j \quad (2b)$$

$$i = \{a, b, c, d, e\}, \quad j = \{d, e\}$$

where  $b$  is the body fixed frame,  $\mathbf{R}$  is the rotation matrix between frame  $b$  and the inertial frame  $O$ ,  $\boldsymbol{\omega}_p$  is the platform angular velocity,  ${}^b \mathbf{I}$  is its inertia matrix, and  $\mathbf{v} = [\dot{x}, \dot{y}, \dot{z}]^T$  is its center of mass (CM) velocity with respect to the inertial frame  $O$ . The subscripts  $i = \{a, b, c\}$  correspond to frictional forces at the three contact points of the platform, and  $i = \{d, e\}$  correspond to the two actuation forces generated by the two vibrating motors. During analysis, equations are simplified due to planar motion.

The actuators are implemented using two vibration DC micromotors (see Fig. 3b), whose dynamics are described by the following equations:

$$\begin{aligned} \ddot{\theta} &= -\frac{b}{J} \dot{\theta} + \frac{k_t}{J} i_L - \frac{mgr \sin\theta}{J} - \frac{c}{J} \\ \dot{i}_L &= -\frac{k_t}{L} \dot{\theta} - \frac{R}{L} i_L + \frac{1}{L} V_{in} \end{aligned} \quad (3)$$

where  $\theta$  is the angle of the motor,  $i_L$  is the current in the windings of the motor,  $R$  is the electrical resistance,  $b$  is the viscous friction,  $c$  is the Coulomb friction,  $k_t$  is the torque constant,  $L$  is the inductance,  $J$  is the eccentric's load inertia and  $V_{in}$  the input voltage. The actuation forces generated by

the motor when its eccentric load rotates are described by the following equations:

$$\begin{aligned} {}^b f_{ix} &= (mr\ddot{\theta} \cos \theta - mr\dot{\theta}^2 \sin \theta) \sin \phi_i \\ {}^b f_{iz} &= -mg - mr\ddot{\theta} \sin \theta - mr\dot{\theta}^2 \cos \theta \end{aligned} \quad (4)$$

where  $\phi_i$  is the angle of the motor axis with respect to the axis of symmetry of the platform.

### III. PULSED ACTUATION

The platform's driving principle presented in [11,12] is based on the Concurrent Operation of Motors (COM). In this mode, both motors operate and depending on the relative sense of rotation of the two actuators, the resultant actuation forces and moments may induce translational or rotational motion to the platform. In practice, mechanical asymmetries give rise to parasitic motions that have to be compensated for, by suitably applying a differential speed between the two motors. According to simulations, when the driving signal is generated by a low-level motor speed controller whose set-points are determined by a high-level platform position controller, the resulting motion has i) a wide mobility range (i.e. is capable for coarse motion as well as fine motion), and ii) a resolution down to a few microns or even to the submicron level [11]. However, when the platform is driven in an open-loop mode, then high motion resolution and high repeatability cannot easily be achieved. Especially during open-loop manipulations, where the platform has to perform short motion steps, operating both motors at the same time is inefficient. Therefore, for open-loop manipulation, a different driving scheme has to be adopted which would be more efficient in terms of control effort, power consumption, motion resolution and repeatability. To this end the Pulsed Actuation (PA) driving mode is proposed and demonstrated in the following paragraph.

#### A. Concept of Pulsed Actuation

Motors are driven electrically by PWM signals. The idea is to set the duty cycle of the PWM to 100% and send a continuous pulse of duration  $T$  to one of the two motors. The speed of the motor will exhibit a first order step response with a mechanical time constant,

$$\tau = \frac{bR + k_t^2}{JR}$$

If the pulse duration  $T$  is sufficiently long, then at some time instant  $t_c$ , the motor speed  $\omega(t_c)$  becomes greater than a critical value  $\omega_c$  and motion is induced. Single motor operation generates both forces and moments and results to a linear displacement  $\Delta x(T)$ ,  $\Delta y(T)$  of the CM and to an angular displacement of the platform  $\Delta \theta(T)$ , whose amplitudes depend on the pulse duration  $T$ . We define a generalized displacement column vector  $\mathbf{y} = [\Delta x(T) \Delta y(T) \Delta \theta(T)]^T$ . This can be written as  $\dot{\mathbf{y}} = f(\mathbf{v})$ , where the function  $f(\bullet)$  involves the dynamics of the platform, and the argument  $\mathbf{v}$  is a control vector with three control elements: *motor name*, *pulse duration*  $T$  and *sense of rotation*. The objective is to construct sequences

of such control vectors, so that the platform exhibits a desired displacement. A single step response of the platform and of the motor, for control vector  $\mathbf{v} = \{\text{Motor A}, T=0.08\text{s}, \text{CW}\}$ , is depicted in Fig. 4.

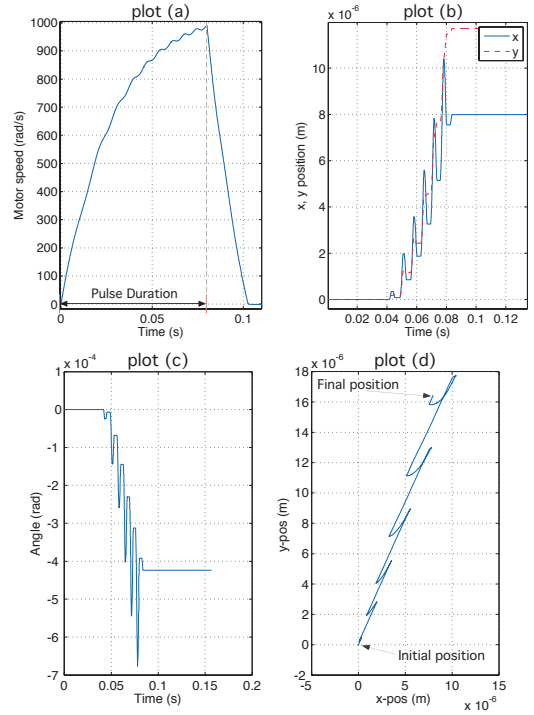


Figure 4. (a) Motor Speed, (b) x, y platform trajectories, (c) Angle platform trajectory, (d) x-y path of the needle tip.

Fig. 4d demonstrates the path described by the tip of a needle attached to the platform. The position of the needle is presented on the drawing shown in Fig. 4a.

During manipulations, the needle's tip moves within the field of view of a video-microscope. The displacement  $\{\Delta x(T), \Delta y(T), \Delta \theta(T)\}$  corresponds to a  $\mathbf{y}_n^O = [\Delta x_n(T) \Delta y_n(T)]^T$  displacement of the needle's tip, calculated by:  $\mathbf{y}_n^O = T_b^O \mathbf{y}_n^b$ , where  $\mathbf{y}_n^b$  is the needle's tip position wrt the body fixed frame, and  $T_b^O$  is the transformation matrix expressing the coordinate transformation between frame  $b$  and the inertial frame  $O$ , (see figure 3a). The norm  $\|\mathbf{y}_n^O\|$ , as a function of the pulse duration  $T$ , is depicted in Fig. 5. It is observed that  $\|\mathbf{y}_n^O\|$  is a monotonic increasing function with respect to  $T$ . Also it is evident that the relationship may be considered linear.

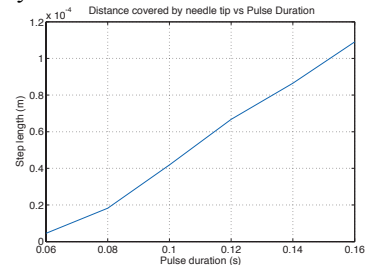


Figure 5. Distance covered by needle as a function of Pulse Duration

## IV. HARDWARE INTEGRATION

### A. Hardware Design

The objectives of the microrobot mechanical design are: i) Miniaturization of dimensions so that a cluster of 3-4 robots can cooperate within a limited workspace such as the workspace under a microscope. ii) The overall cost of the microrobot components should be as small as possible. iii) The design should comprise as few parts as possible for simplicity and for rapid assembly. iv) The components should be readily available in the market.

The first prototype has been designed and built according to the above objectives, see Fig. 6a. The base is made of a cylindrical solid piece of Plexiglas, within which the two actuators have been integrated. Also into the same piece of Plexiglas a strain gauge is installed onto a flexible copper sheet with dimensions (11x8x0.1mm) and rectangle geometry. On this copper sheet a needle (cantilever) has been mounted as shown in Fig6b. The strain gauge measures the forces applied on the needle. The actuators speed is measured using a non-contact sensor (optoreflectors) per motor. These have miniature dimensions and can be placed in close proximity to the eccentric mass. This way a pulse per revolution is obtained. The rest of the parts used in the mechanical assembly are removable masses, spacers and PCBs. Duration of manufacturing is less than 2 days and the machinery required is essentially handheld tools. Table I lists some of the most critical design parameters.

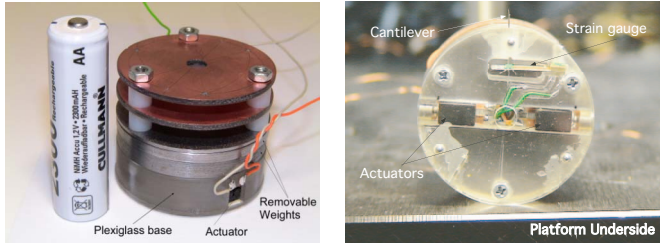


Figure 6. a) Mechanical parts of platform b) Strain gauge installation

TABLE I DESIGN PARAMETERS

Parameter	Value	Parameter	Value
r	0.00177[m]	L	0.04 [m]
m	0.00021[kg]	H	0.004 [m]
M	0.1 [kg]	M	0.5

Where  $l$  is the radius of the platform,  $h$  is the height of the CM and  $\mu$  is the coefficient of friction. For the rest of the parameters refer to Fig. 1.

### Electronic System Design and Integration

The objective of the electronic subsystem design is: (i) to allow for remote tetherless microrobot operation, (ii) to provide power autonomy, which in effect means that four on-board coin-battery cells should provide sufficient amper-hours for completing successfully a predefined manipulation task, (iii) to comply with the hardware dimensional constraints, meaning that the electronics should occupy the least possible space.

Untethered driving is considered a key concept for the microrobot design. Any wire connecting the robot to a power

supply, or with a processing and a communication unit, exerts moments on the mobile platform and severely affects the motion accuracy and repeatability. Furthermore in the case of a multi robot scenario, the entanglement of wires substantially reduces the flexibility of the microrobotic system. The greatest challenge in terms of electronics integration is to select components and design a circuit topology, which can meet the stringent requirements of the dimensional constraints. To this end, Surface Mount Device (SMD) technology was employed in order to minimize the total space occupied by the components.

The first design iteration of the electronic system consists of three separate printed circuit boards (PCB) whose geometry is dictated by that of the mechanical subsystem, see Fig. 6. These PCBs are interconnected to each other through suitable sockets and the total circuit is assembled in a three stage compact topology. Starting from the bottom board, (1<sup>st</sup> level), the circuit consists of the driving circuitry and of a signal conditioning circuit for processing force sensor measurements. The middle board, (2<sup>nd</sup> level), hosts the on-board processing unit, auxiliary signal conditioning circuits for speed (rpm) sensors, and a programming header. This forms the system control logic unit.

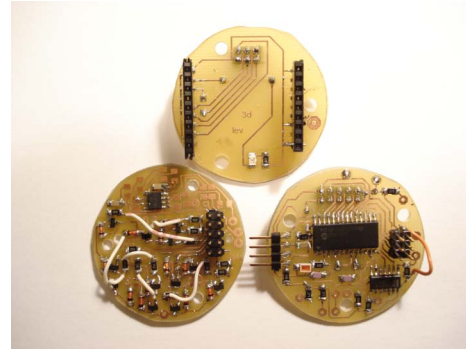


Figure 7. The separate circuit boards of the first prototype, from left to right: 1st stage, 3rd stage and 2nd stage

Finally the top board, (3<sup>rd</sup> level), is devoted to the wireless communication subsystem, and comprises a socket with all the necessary signals to establish communication with a dedicated transceiver module (434Mhz band or RF Bluetooth). For reducing the effects of a top-heavy design, batteries are securely installed at the lowest level, i.e. between the base of the platform and the first board. The architecture implemented in the three levels is shown schematically in Fig. 7.

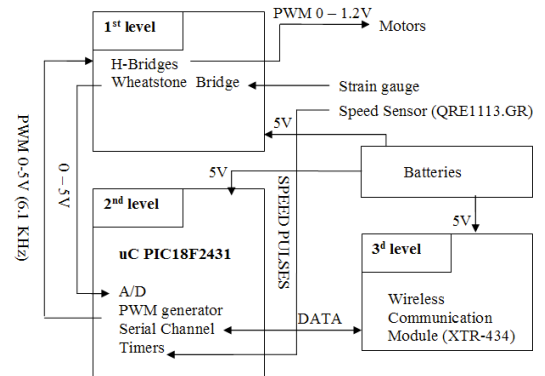


Figure 8. Data flow and functionality of the electronic modules.

### B. Description of each module

*First level:* Has 3 simple H-bridge configuration circuits. These were built in-house using discrete components since there is no commercially available single IC solution providing an H-bridge at 1.2V. Each bridge has 4 SMD small signal transistors equivalent to the BC547 transistor with protection diodes. They all share a common voltage DC bus of 1.2V for power supply and every transistor is driven through a resistor connected directly to the appropriate microcontroller pin. The H-bridges are driven in a hard-switching mode, meaning that the upper switch of the one transistor pair and the lower switch of the other transistor pair share the same PWM signal, and the other two switches share the complementary PWM signal. Employing this technique only two pins of the microcontroller are devoted to each H-bridge. When both actuators operate at a nominal speed, i.e. about 7000 RPM, the total electrical consumption is less than 250 mW, of which 100 mW are consumed by the actuators and the H-bridges and approximately 150 mW are consumed by the PIC microcontroller.

A second circuit placed onto this board implements a common Wheatstone bridge using two operational amplifiers of an LM358 IC and a subsequent filter for noise reduction. This way the strain gauge sensor, installed within the Plexiglas part of the platform, can feed the microcontroller with the appropriate voltage levels to measure forces exerted by the platform onto an object.

*Second level:* This hosts the core of the electronic subsystem, which is based on the motor control oriented microcontroller from Microchip, PIC 18F2431. This small microcontroller shares the features of a usual general-purpose 8bit micro processing unit and the special characteristics of motor control drivers. The microcontroller has built-in specialized features for providing 3-phase output. It offers three pairs of PWM outputs. Each pair provides complementary square wave output signals facilitating the soft-switching mode of operation of the H-bridge circuits. Applying a 10 MHz external crystal, the system clock goes up to 10 MIPS. The switching frequency is 6.1 KHz providing 10 bits of resolution for each direction of rotation. This switching frequency is high enough so that PWM pulses do not affect the motor torque.

Two internal timers are used as counters for measuring the speed of the motors in a predefined time base. Motor speed feedback is achieved using the sensor QRE1113.GR in SMD form, an object reflector comprising a LED diode and a phototransistor in the same package. This component was favored first of all because: (i) it provides non-contact means of measurement and thus does not affect motor characteristics, (ii) it has very small dimensions (1.6x4.5x3.3mm), and (iii) It operates on a current consumption down to 5 mA and consumes no more than 50mW. This opto-reflector is placed at 0.8 to 1 mm distance from the motor's eccentric load. During each motor rotor rotation, the sensor generates a pulse type output signal, which is fed into a Schmitt-Trigger inverter gate

(CD40106) to avoid signal disturbances from noise; finally the clear pulse is applied to the microcontroller for further processing by the counters. The bandwidth of the opto-reflector is about 25 kHz.

*The third stage:* This stage of the PCB boards is devoted to the wireless communication, between a control PC, used for control, and the microrobot. The communication is accomplished through a full duplex channel. To this end, a transceiver is installed on the control PC and another one on the microrobot. These transceivers translate the serial data of a COM port into modulated data signals of a specific frequency (434 MHz or 2.4 GHz for Bluetooth) and vice versa. Consequently the microcontroller accepts data in the EUSART module, and sends data back to the PC for feedback (force signal 0-5V from the strain gauge). The signals that are transmitted from the central PC to the platform are a sequence of control vectors  $\mathbf{y}$  that drive the platform. The signal sent from the platform to the control PC is the force feedback generated by the strain gauge. The need for force feedback arises from specific micro assembly tasks (e.g. peg in hole).

To achieve high fidelity force feedback, a high sampling rate of about 1 kHz is required for closing the loop and successfully accomplishing force control tasks. A communication protocol with predefined commands of control and a baud rate up to 57.6 Kbps is sufficient for establishing the required communication channel. Another design aspect of the third stage electronic circuit is that it provides a standard interface to match the majority of wireless modules: transmit and receive signals, and an enable option for each of them. Currently, the XTR-434 transceiver module from AUREL is used. In the final design iteration wireless communication module will be selected according to stringent criteria on power consumption, baud rate, and dimensions.

Fig. 9 demonstrates the microrobot after the first two levels of electronics have been assembled and mounted on the platform. The top level i.e. the one with the communication electronics has not been added yet.

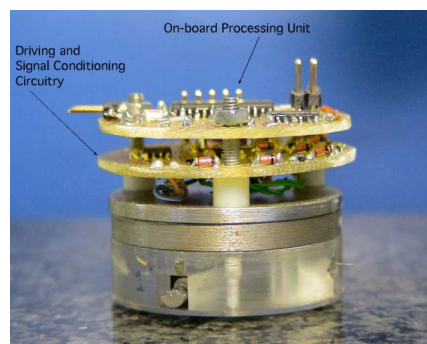


Figure 9. Hardware integration.

## V. PULSED ACTUATION EXPERIMENT

Experiments have been conducted in order to assess the results of the analysis presented in paragraph III and to demonstrate the fine motion capabilities of the platform. The experimental set-up is demonstrated in Fig. 10.

The microscope has a maximum field of view of 1x1mm and a minimum 330x330 $\mu\text{m}$ . The video camera pixel size is selected so that the accuracy of the system is approximately 2 $\mu\text{m}$ . Image processing algorithms have been implemented so that the recorded path described by the needle tip can be tracked and plotted off-line.

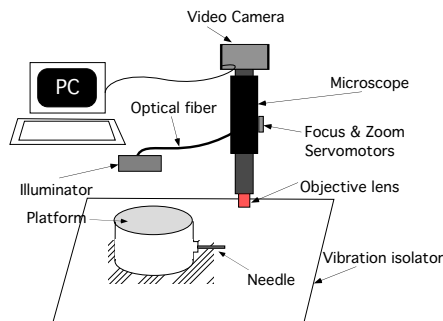


Figure 10. Experimental set-up

In this experiment seven successive positive driving pulses of 1V and duration 200-300 ms were dispatched to motor D (see Fig. 3a). The platform's CM moved towards the positive x-axis, towards the positive y-axis and the platform exhibits a negative rotation about the z-axis. The path described by the needle tip was recorded by the microscope and is depicted in Fig. 11. The needle's initial and final positions are presented in the photos in Fig. 12a and b respectively. It can be seen that the experimental results are qualitatively in accordance with the simulation results presented in paragraph III. It should be noted that the refresh rate of the camera is not sufficient to capture the oscillations performed by the platform during each step. Therefore, the overshoot predicted by the simulation results demonstrated in Fig. 4 is not visible in the experimental results depicted in Fig 11.

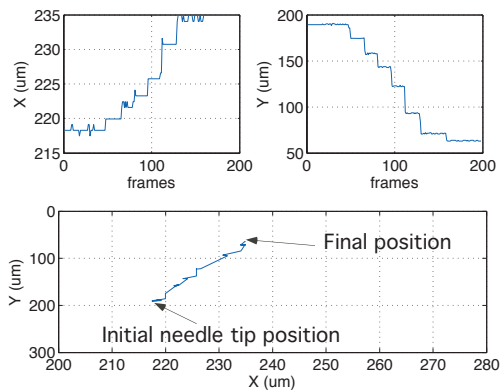


Figure 11. Experimental results of pulsed actuation.

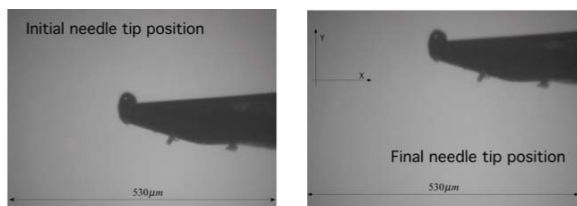


Figure 12. Needle tip: a) Initial position b) Final position

## VI. CONCLUSIONS

The paper presented a new driving principle that can be employed by microrobotic platforms whose actuation mechanism is based on vibrating motors. It was demonstrated through simulations and experimental results that this driving principle results to a controlled motion composed of a sequence of discrete steps with precision down to a few microns. The driving procedure is most appropriate for manipulation operations where the distance to be covered is relatively small and high resolution and repeatability are required. Furthermore the paper presented an overview of the hardware assembly process giving emphasis on the integration of the electronic systems and demonstrated the simplicity of the design and of the hardware integration process.

## REFERENCES

- [1] A. Kortschack, A. Shirinov, T. Truper, S. Faticow, "Development of Mobile Versatile Nanohandling Microrobots: Design, Driving Principles, Haptic Control," *Robotica*, p. 419-434, July 2005.
- [2] A. Tafazzoli, C. Pawashe and M. Sitti, "Force controlled Microcontact Printing using Microassembled Particle Templates," *IEEE International Conference on Robotics and Automation (ICRA2006)*, Orlando, USA.
- [3] Yu Sun, K. Kim, R.M. Voyles, B.J. Nelson, "Calibration of Multi-Axis MEMS Force Sensors Using the Shape from Motion," *IEEE International Conference on Robotics and Automation (ICRA2006)*, Orlando, USA.
- [4] Jean-Marc Breguet, Reymond Clavel, "Stick and Slip Actuators: design, control, performances and applications," *International Symposium on Micromechanics and Human Science (MHS)*, (Nagoya), 1998, 89-95.
- [5] Schmoekkel, F., and Fatikow, S, "Smart Flexible Microrobots for Scanning Electron Microscope (SEM) Applications," *Journal of Intelligent Material Systems and Structures*, Vol. 11, No. 3, 2000, pp. 191-198.
- [6] Büchi Roland, Zesch Wolfgang, Codourey Alain, "Inertial Drives for Micro- and Nanorobots: Analytical Study," *Proceedings of SPIE Photonics East '95: Proc. Microrobotics and Micromachanical Systems Symposium*, Vol. 2593, Philadelphia, PA, Lynne E. Parker - Bellingham, WA, SPIE, 1995
- [7] Büchi Roland, Zesch Wolfgang, Codourey Alain, "Inertial Drives for Micro- and Nanorobots: Analytical Study," *Proceedings of SPIE Photonics East '95: Proc. Microrobotics and Micromachanical Systems Symposium*, Vol. 2593, Philadelphia, PA, Lynne E. Parker - Bellingham, WA, SPIE, 1995.
- [8] Martel Sylvain et al., "Three-Legged Wireless Miniature Robots for Mass-scale Operations at the Sub-atomic Scale," *Proc. 2001 IEEE International Conference on Robotics & Automation*, Seoul, Korea, May 21-26, 2001, pp. 3423-3428.
- [9] J. Brufau, M. Puig-Vidal, et. al, MICRON: Small Autonomous Robot for Cell Manipulation Applications, Proc. of the IEEE International Conference on Robotics & Automation, Barcelona, Spain, April 18-22, 2005.
- [10] P. Vartholomeos, S. Loizou, M. Thiel, K. Kyriakopoulos and E. Papadopoulos, "Control of the Multi Agent Micro-Robotic Platform MiCRoN," *IEEE International Conference on Control Applications*, Munich, Germany, October 2006, (To Appear)
- [11] P. Vartholomeos and E. Papadopoulos, "Analysis, Design and Control of a Planar Micro-robot Driven by Two Centripetal-Force Actuators," *IEEE International Conference on Robotics and Automation 2006 (ICRA2006)*, Orlando USA.
- [12] P. Vartholomeos and E. Papadopoulos, "Dynamics, Design and Simulation of a Novel Microrobotic Platform Employing Vibration Microactuators," *Journal of Dynamic Systems, Measurement and Control*, ASME, March 2006.
- [13] L. Sciacivico and B. Siciliano, "Modelling and Control of Robot Manipulators," Springer 2003.